

1 The impact of wildfire smoke on ozone production in an urban area: insights from field 2 observations and photochemical box modeling

3
4 Matthew Ninneman^{a,*}, Daniel A. Jaffe^a

5
6 ^aSchool of Science, Technology, Engineering and Mathematics, University of Washington
7 Bothell, 18115 Campus Way NE, Bothell, WA, 98011, USA

8 * Corresponding author. *E-mail address*: mn77@uw.edu
9

10 Abstract

11
12 This study examines the effect of wildfire smoke on ozone (O₃) production at an urban
13 site in Bakersfield, CA. We used data from smoky and non-smoky weekdays in summer 2018.
14 Median surface observations across the smoky and non-smoky weekdays showed that morning
15 and afternoon O₃ concentrations were mainly affected by local photochemistry. Observed
16 daytime median concentrations of O₃, particulate matter with diameters less than 2.5 μm (PM_{2.5}),
17 and carbon monoxide (CO) were approximately 8 parts per billion (ppb), 8 micrograms per cubic
18 meter (μg m⁻³), and 40 ppb higher, respectively, on the smoky weekdays. The observed median
19 sum of the daily-average concentrations of volatile organic compounds (ΣVOCs) was
20 approximately 10 ppb greater on the smoky weekdays. Measured daytime median NO_x levels
21 were almost identical on the smoky and non-smoky weekdays, indicating that the enhancement
22 in NO_x due to smoke was negligible. We used the Framework for 0-D Atmospheric Modeling
23 (FOAM) box model to examine the photochemical processes on the smoky and non-smoky
24 weekdays. The maximum model-predicted instantaneous O₃ production rates (P_{O₃}) were about
25 18 and 9 ppb h⁻¹ on the smoky and non-smoky weekdays, respectively. Model sensitivity tests
26 showed that (1) O₃ was sensitive to both NO_x and VOCs on the smoky weekdays, (2) aldehydes
27 significantly affected O₃ formation when wildfire smoke was overhead, and (3) the O₃
28 production regime on the non-smoky weekdays was likely NO_x-saturated. Our results suggest
29 that a combination of anthropogenic VOC and NO_x reductions will be the most effective strategy
30 for decreasing O₃ on typical non-smoky days. In contrast, due to the high VOC levels in smoke
31 plumes, only reductions in NO_x are expected to have a significant effect on lowering O₃
32 concentrations on typical smoky days.
33

34 Keywords: Wildfires, Smoke, Ozone, Volatile organic compounds, Nitrogen oxides, Box model
35

36 1. Introduction

37
38 Over the past two decades, the annual area burned in the U.S. by wildland fires has
39 increased dramatically. Data from the National Interagency Fire Center (www.nifc.gov) show
40 that there have been 10 years with more than 3.2 million hectares (ha) burned since 1960, and all
41 have occurred since 2004. The U.S. currently experiences a strong fire season (i.e., more than 3.2
42 million ha burned) approximately every other year. This increase in wildfire activity is due to
43 climatological factors (e.g., drought, higher summertime temperatures, earlier snowmelt, etc.),
44 forest management, and human ignitions (Aldersley et al., 2011; Balch et al., 2017; Decker et al.,
45 2019; Dennison et al., 2014; Kitzberger et al., 2007; Littell et al., 2009; Miller and Safford, 2012;
46 Westerling et al., 2006). Since wildfires are expected to increase in the future (Moritz et al.,

47 2012; Pechony and Shindell, 2010; Spracklen et al., 2009; Val Martin et al., 2015), it is essential
48 to understand how they impact urban air quality and photochemistry.

49 Wildfires emit large but highly variable amounts of carbon monoxide (CO), particulate
50 matter with diameters less than 2.5 μm ($\text{PM}_{2.5}$), volatile organic compounds (VOCs), and oxides
51 of nitrogen (NO_x = nitric oxide (NO) + nitrogen dioxide (NO_2)); except for $\text{PM}_{2.5}$, all are ozone
52 (O_3) precursors (Akagi et al., 2011; Andreae, 2019; Lindaas et al., 2020). Emissions from these
53 fires have had major air quality implications. Laing and Jaffe (2019) show that fires in 2017 and
54 2018 led to millions of Americans being exposed to some of the highest-ever $\text{PM}_{2.5}$
55 concentrations measured in the U.S. Many sites had daily-average $\text{PM}_{2.5}$ concentrations
56 exceeding 500 $\mu\text{g m}^{-3}$. McClure and Jaffe (2018a) found that smoke from these fires was
57 changing the general long-term downward trend in $\text{PM}_{2.5}$ to an upward trend for the policy-
58 relevant 98th percentile days in much of the western U.S. Gong et al. (2017) found that smoke
59 can increase the maximum daily 8-hour average (MDA8) O_3 by up to 40 ppb at some locations,
60 often leading to an exceedance of the O_3 National Ambient Air Quality Standard (NAAQS) of 70
61 ppb.

62 Due to large variations in the emissions, plume injection heights, and photochemical
63 processing associated with wildfires, it is challenging to use regional and global air quality
64 models to examine the effect of wildfire smoke on urban O_3 production. Typical Eulerian grid
65 models cannot capture the detailed and rapid photochemical processes that occur in a smoke
66 plume. The most common problem in these applications appears to be significant over-
67 production of O_3 due to rapid plume dilution into a model grid cell or an inadequate chemical
68 mechanism (e.g., Zhang et al., 2014; Baker et al., 2016; Lu et al., 2016). Model underpredictions
69 have also been reported in a few cases (e.g., Singh et al., 2012; Cai et al., 2016). These
70 underpredictions are likely due to modeled meteorology failing to transport smoke to the
71 receptor location and/or inadequate fire emissions.

72 Due to the difficulty in modeling smoke-produced O_3 , several studies have used
73 observational analyses (e.g., Buysse et al., 2019; Dreessen et al., 2016; Lindaas et al., 2017;
74 McClure and Jaffe, 2018b; Rubio et al., 2015) or statistical modeling (Jaffe et al., 2004, 2013; Lu
75 et al., 2016; Gong et al., 2017; McClure and Jaffe, 2018b) to analyze O_3 from fire precursors.
76 Buysse et al. (2019) assessed the impact of wildfire smoke on O_3 in 18 western U.S. cities using
77 surface observations of $\text{PM}_{2.5}$, NO_x , and O_3 . They also used the NOAA Hazard Mapping System
78 Fire and Smoke Product (HMS FSP) to detect overhead smoke influence. They found that $\text{PM}_{2.5}$
79 and O_3 were usually enhanced on days with smoke, while NO_x did not exhibit a consistent
80 enhancement. However, $\text{PM}_{2.5}$ and O_3 on smoke days were nonlinearly related, with O_3
81 increasing at low to moderate $\text{PM}_{2.5}$ concentrations, reaching a maximum when $\text{PM}_{2.5}$
82 concentrations were approximately 30-50 $\mu\text{g m}^{-3}$, remaining enhanced up to $\text{PM}_{2.5}$
83 concentrations of about 100 $\mu\text{g m}^{-3}$, and decreasing at higher $\text{PM}_{2.5}$ concentrations. The authors
84 also found that the morning rate of O_3 increase ($d\text{O}_3/dt$) was higher and the NO/NO_2 ratios were
85 lower on smoke-influenced days (Buysse et al., 2019). These results suggest that the elevated O_3
86 on smoke-influenced days in urban areas is likely a result of enhanced in-situ photochemical
87 production, rather than direct transport of O_3 already in the smoke plume.

88 Statistical modeling identifies the relationship between O_3 and meteorological variables
89 (temperature, winds, humidity, etc.) for non-smoke days (e.g., Camalier et al., 2007) and then
90 uses this relationship to examine observed O_3 on days with and without smoke. This approach
91 has been used in numerous studies to quantify the additional amount of O_3 produced by fire
92 precursors (e.g., Jaffe et al., 2004, 2013; Lu et al., 2016; Gong et al., 2017; McClure and Jaffe,

93 2018b). This method is also considered acceptable for quantifying smoke impacts on surface O₃
94 for exceptional event demonstrations (U.S. EPA, 2016). A typical approach uses Generalized
95 Additive Models (GAMs), which are a form of machine learning. Using GAMs, Gong et al.
96 (2017) found that MDA8 O₃ values were on average 3-8 ppb higher on smoke days in eight
97 western U.S. urban areas, with a maximum O₃ enhancement due to wildfire precursors of 40 ppb.
98 The authors also found that 19% of the days with MDA8 O₃ exceeding 75 ppb were influenced
99 by smoke, even though smoke days comprised only a small fraction (4.1%) of all days analyzed
100 (Gong et al., 2017). However, while this approach can provide an estimate of the additional O₃
101 due to fire emissions, it does not provide much information about the O₃ formation mechanisms
102 or factors controlling O₃ production.

103 Given the challenge of modeling smoke photochemistry with grid models, several studies
104 have applied 0-D photochemical box models to this problem (Mason et al., 2006; Alvarado et al.,
105 2015; Müller et al., 2016; Coggon et al., 2019; Decker et al., 2019). Although there are
106 differences in the methodologies, each of these studies was reasonably successful at modeling O₃
107 production in a smoke plume. Key to this success was the ability to link the model to emission
108 data and to use a chemical mechanism that captured the essential chemical features. Despite
109 these successes, to our knowledge, this method has not been applied to smoke in urban areas,
110 where O₃ exceedances have significant regulatory implications.

111 O₃ production is sensitive to either VOCs, NO_x, or both, and O₃ control strategies have
112 focused on reducing the concentrations of the limiting reagent. Regions with a high VOC/NO_x
113 ratio are in a NO_x-sensitive O₃ production regime, and regions with a low VOC/NO_x ratio are in
114 a NO_x-saturated O₃ production regime (e.g., Sillman, 1999; Farmer et al., 2011; Pusede and
115 Cohen, 2012; Qian et al., 2019). Emissions from wildland fires have relatively high VOC/NO_x
116 ratios (e.g., molar ratios of 25-100; Akagi et al., 2011; Andreae, 2019), so these emissions can be
117 particularly important when mixed into a NO_x-rich urban area. Overall, correctly diagnosing the
118 O₃ production environment during smoke-influenced periods is important when assessing the
119 impact of smoke on O₃ in an urban area. We also note the importance of weekday/weekend
120 differences in NO_x concentrations on O₃ production (Baidar et al., 2015; de Foy et al., 2020).

121 To address the research gaps highlighted above, we investigated the effect of wildfire
122 smoke on O₃ production at an urban site in Bakersfield, CA. To avoid complications due to
123 weekday/weekend effects, we examine O₃ production on smoky and non-smoky weekdays in
124 summer 2018. The analysis was performed using a combination of surface measurements and a
125 0-D photochemical box model.

126

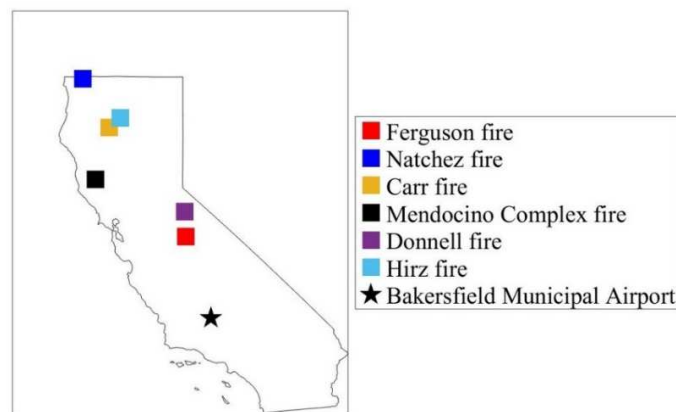
127 **2. Materials and Methods**

128

129 The Bakersfield Municipal Airport site (BMA; 35.33 °N, 119.00 °W; AQS ID
130 060292012) is located in the city of Bakersfield, California, and it is operated by the San Joaquin
131 Valley Unified Air Pollution Control District. Some of the measurements made at BMA include
132 O₃, carbon monoxide (CO), oxides of nitrogen (NO_x = nitric oxide (NO) + nitrogen dioxide
133 (NO₂)), a suite of approximately 50 volatile organic compounds (VOCs), air temperature (T_{air}),
134 barometric pressure (BP), and relative humidity (RH). Since particulate matter with diameters
135 less than 2.5 μm (PM_{2.5}) is not measured at BMA, PM_{2.5} data from the California Avenue site
136 (35.36 °N, 119.06 °W; AQS ID 060290014) were used. The California Avenue site is located
137 approximately 6 km to the northwest of BMA, and it is operated by the California Air Resources
138 Board.

139 Measurements of the above parameters were used to help investigate the impact of
140 wildfire smoke on morning (6:00-11:00 LST) and afternoon (11:00-17:00 LST) O₃ formation at
141 BMA during summer (July-August) 2018. Hour-averaged O₃, CO, NO_x, PM_{2.5}, T_{air}, BP, and RH
142 data were obtained from EPA AirNow-Tech (<https://www.airnowtech.org/>). Daily-averaged
143 speciated VOC data collected by canisters every three hours were retrieved from the EPA Air
144 Data system (<https://www.epa.gov/outdoor-air-quality-data>). While the VOC data are typical for
145 state monitoring systems, it should be noted that wildfire smoke contains hundreds of VOCs that
146 are not usually measured in this network. Thus, it is likely that VOC concentrations are
147 significantly underestimated for the smoke days.

148 The effect of wildfire smoke on O₃ production at BMA was assessed using data collected
149 on 13 smoky weekdays and 20 non-smoky weekdays in July and August 2018. The dates of the
150 smoky weekdays were July 6, 24-27, and 30-31 and August 2, 6, 8-10, and 15. The dates of the
151 non-smoky weekdays were July 3-4, 9-10, 12-13, 16, and 18-20 and August 3, 14, 17, 20-21, 23-
152 24, 27, and 29-30. These days were selected for analysis because each had measurements of O₃,
153 CO, VOCs, NO_x, PM_{2.5}, T_{air}, BP, and RH. A combination of surface PM_{2.5} measurements,
154 surface CO measurements, and imagery from the NOAA Hazard Mapping System Fire and
155 Smoke Product (HMS FSP; <https://www.ospo.noaa.gov>) were used to distinguish between the
156 smoky and non-smoky weekdays. We focused on weekdays since numerous studies have
157 reported higher concentrations of O₃ precursors (i.e., VOCs and NO_x) on weekdays than on
158 weekends in southern California (e.g., Blanchard and Tanenbaum, 2003; Fujita et al., 2003).
159 Therefore, weekends were excluded from the analysis so that any differences in O₃ formation
160 chemistry on the smoky versus non-smoky days could be more readily attributed to wildfire
161 smoke. The overhead smoke on the smoky weekdays was likely due in part to the large Ferguson
162 (about 39,000 ha burned), Natchez (about 15,000 ha burned), Carr (about 93,000 ha burned),
163 Mendocino Complex (about 186,000 ha burned), Donnell (about 15,000 ha burned), and/or Hirz
164 (about 19,000 ha burned) fires burning north of BMA. The locations of each of these fires
165 relative to BMA are shown in Fig. 1.
166



167
168 **Fig. 1. Site and Wildfire Map** Map of California showing the locations of the Bakersfield
169 Municipal Airport (BMA) site and the Ferguson, Natchez, Carr, Mendocino Complex, Donnell,
170 and Hirz fires.
171

172 The measurements listed above were used to constrain the Framework for 0-D
173 Atmospheric Modeling photochemical box model (F0AM; Wolfe et al., 2016). Since none of the
174 chemical mechanisms in F0AM include heterogeneous chemistry, PM_{2.5} was not used as a model

175 constraint. Version 3.3.1 of the Master Chemical Mechanism (MCM v3.3.1,
176 <http://mcm.leeds.ac.uk/MCM>; Jenkin et al., 1997, 2003, 2015; Bloss et al., 2005; Saunders et al.,
177 2003) was used to drive the model chemistry. One 24-hour simulation was conducted from 0:00-
178 23:00 LST for both the smoky and non-smoky weekdays to investigate the average impact of
179 wildfire smoke on O₃ formation chemistry. Both simulations had a 10-minute integration time
180 for each model time step, and a 2-day model spin-up was performed to ensure that the initial
181 conditions had little to no effect on the modeling. Observed hourly median T_{air}, BP, and RH
182 across the smoky or non-smoky weekdays were used to initialize the meteorology in F0AM for
183 each time step of the simulations. All observed medians of the daily-average VOC
184 concentrations for the smoky weekdays were scaled upward by 30% to account for unmeasured
185 VOCs emitted by wildfires. The individual VOCs used to constrain F0AM for the smoke and
186 non-smoke simulations are shown in Table S1. O₃, CO, VOCs, and methane (CH₄) were
187 initialized at the beginning of the smoke and non-smoke simulations (i.e., 0:00 LST) using (1)
188 the observed median O₃ and CO concentrations at 0:00 LST across the smoky or non-smoky
189 weekdays, (2) the observed medians of the daily-average VOC concentrations, and (3) an
190 assumed CH₄ concentration of 1850 ppb. After O₃, CO, VOCs, and CH₄ were initialized at 0:00
191 LST for the smoke and non-smoke model runs, their concentrations varied freely for the rest of
192 the 24-hour simulations. Observed hourly median NO_x concentrations across the smoky and non-
193 smoky weekdays were used to initialize F0AM for all hours of the smoke and non-smoke
194 simulations. Specifically, the total NO_x concentrations were set at the beginning of each model
195 time step, while the NO/NO₂ ratio was calculated by the model chemistry.

196 Fixed background O₃, CO, and VOC concentrations were prescribed for the smoky and
197 non-smoky weekdays. Background O₃ and CO values were specified by determining daily
198 median concentrations on the smoky and non-smoky weekdays. Ultimately, background O₃ and
199 CO concentrations of 45 and 300 ppb, respectively, were prescribed for the smoky weekdays,
200 and background O₃ and CO concentrations of 40 and 240 ppb, respectively, were prescribed for
201 the non-smoky weekdays. Background VOC concentrations for the smoky and non-smoky
202 weekdays were assumed to be equal to the initialized values (Table S1).

203 Photolysis rates were calculated as a function of solar zenith angle, elevation of BMA
204 (117 m a.s.l.), albedo (0.15), and overhead O₃ column (300 DU) using lookup tables provided in
205 F0AM. The lookup tables are determined using (1) literature-derived cross sections and quantum
206 yields and (2) solar spectra from version 5.2 of the National Center for Atmospheric Research
207 Tropospheric Ultraviolet and Visible (NCAR TUV) radiation model (Wolfe, 2020). We note that
208 the model-calculated photolysis rates were not adjusted for cloud cover or aerosol optical depth
209 (AOD). Sky cover data from Meadows Field Airport (35.43 °N, 119.06 °W; about 12 km north-
210 northwest of BMA) indicate that there was negligible cloud cover on the smoky and non-smoky
211 weekdays (IEM, 2021). In addition, Baylon et al. (2018) reported a minimal impact of AOD on
212 photolysis rates at AOD values up to 0.6, and the daily AODs measured by the Moderate
213 Resolution Imaging Spectroradiometer (MODIS) Aqua satellite on the smoky weekdays in
214 Bakersfield had a median value of approximately 0.4 (data not shown).

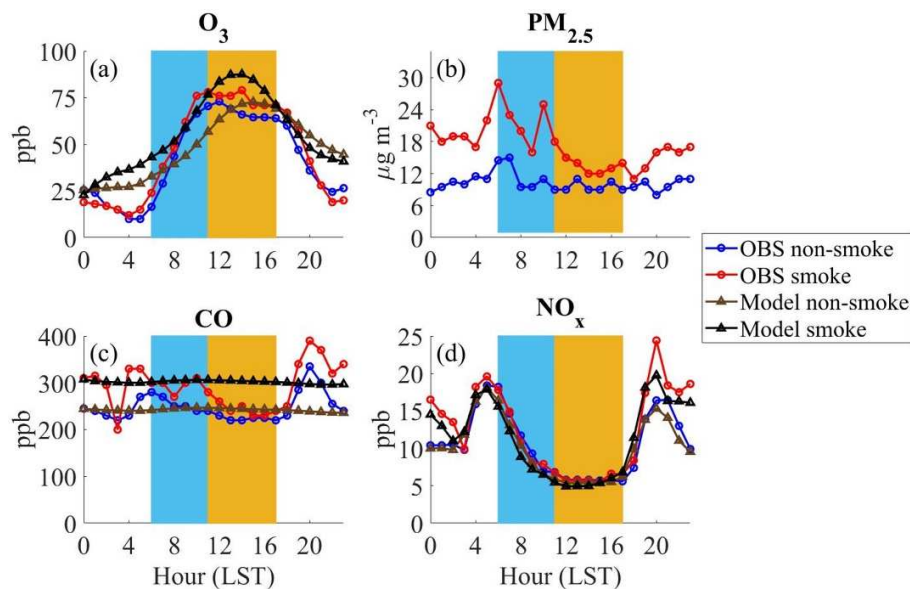
215 Physical processes were accounted for in F0AM by deriving a first-order dilution rate
216 (K_{dil}). K_{dil} was found following an approach adapted from McDuffie et al. (2016) and Ninneman
217 et al. (2020). Namely, different K_{dil} values were tested to determine the best fit of the model-
218 predicted afternoon O₃ concentrations to the observed values. The K_{dil} values that yielded the
219 best fit to the observed afternoon O₃ concentrations for the smoky and non-smoky weekdays
220 were 1×10^{-4} and $3 \times 10^{-5} \text{ s}^{-1}$, respectively. These K_{dil} values also led to reasonable agreement

221 between modeled and measured NO_x concentrations on the smoky and non-smoky weekdays
 222 (Fig. 2 and Table S2). However, we note that the model did not predict the observed decrease in
 223 afternoon CO levels, especially on the smoky weekdays. Since CO is highly influenced by
 224 transport and emissions, this was likely due in part to the lack of upwind measurements to set the
 225 background concentrations of CO and its precursors.

226 To help assess O_3 production at BMA on the smoky and non-smoky weekdays, model-
 227 predicted instantaneous O_3 production rates (P_{O_3}) were examined using Eq. (1) (e.g., Thornton et
 228 al., 2002):

$$229 \quad P_{\text{O}_3} = k_{\text{HO}_2+\text{NO}} [\text{HO}_2][\text{NO}] + \sum_i k_{\text{RiO}_2+\text{NO}} [\text{RiO}_2][\text{NO}], \quad (1)$$

230
 231 where $k_{\text{HO}_2+\text{NO}}$ is the rate constant for the reaction of hydroperoxyl radical (HO_2) with NO , and
 232 $k_{\text{RiO}_2+\text{NO}}$ is the rate constant for the reaction of speciated organic peroxy radicals (RiO_2) with NO .
 233 P_{O_3} differs from the net O_3 production rate in that it does not account for O_3 loss pathways,
 234 mainly surface deposition, chemical loss, and advection. Model sensitivity tests were performed
 235 to investigate the effect of VOCs and/or NO_x on P_{O_3} and O_3 on the smoky and non-smoky
 236 weekdays. All VOC sensitivity tests were conducted by varying the initial and background VOC
 237 concentrations without changing the other model inputs. All NO_x sensitivity tests were
 238 conducted by varying the initialized NO_x concentrations without changing the other model
 239 inputs. Initialized NO_x concentrations and initial and background VOC concentrations were the
 240 only model inputs that were changed for sensitivity tests examining the impact of both NO_x and
 241 VOCs on P_{O_3} and O_3 . The results of these sensitivity tests will be presented and discussed in the
 242 next section.
 243
 244



245
 246 **Fig. 2. Model Predictions and Surface Observations** Hourly modeled concentrations and/or
 247 hourly median observations of (a) O_3 (ppb), (b) $\text{PM}_{2.5}$ ($\mu\text{g m}^{-3}$), (c) CO (ppb), and (d) NO_x (ppb)
 248 on the smoky and non-smoky weekdays. O_3 , CO , and NO_x were measured at BMA. $\text{PM}_{2.5}$ was
 249 measured at the California Avenue site, which is approximately 6 km to the northwest of BMA.
 250 $\text{PM}_{2.5}$ was not modeled, as discussed in section 2. Morning (6:00-11:00 LST) and afternoon
 251 (11:00-17:00 LST) hours are denoted by the light blue and gold shading, respectively.

252 **3. Results and Discussion**

253

254

255 Observed hourly median and/or hourly modeled O₃, PM_{2.5}, CO, and NO_x concentrations
 256 for the smoky and non-smoky weekdays are shown in Fig. 2. Measured O₃ concentrations on the
 257 smoky and non-smoky weekdays increased rapidly from 24 to 78 ppb and 17 to 71 ppb,
 258 respectively, in the morning, reaching a maximum of 79 and 73 ppb, respectively, in the early
 259 afternoon. During daytime hours (6:00-17:00 LST), observed O₃ concentrations were
 260 approximately 8 ppb greater on smoky weekdays (Table 1). Since there were no corresponding
 261 increases in the observed morning PM_{2.5} and CO concentrations, local photochemistry was likely
 262 the main factor influencing measured O₃ levels on the smoky and non-smoky weekdays. On the
 263 smoky weekdays, observed daytime PM_{2.5} values were about 8 μg m⁻³ higher, observed daytime
 264 CO levels were approximately 40 ppb greater, and the observed median sum of the daily-average
 265 concentrations of volatile organic compounds (ΣVOCs) was approximately 10 ppb greater (Table
 266 1). The above differences in the measured concentrations of O₃, PM_{2.5}, CO, and ΣVOCs were
 267 statistically significant (p < 0.05; Table 1). Differences in observed daytime NO_x concentrations
 268 on the smoky versus non-smoky weekdays were negligible and statistically insignificant (Fig. 2d
 269 and Table 1), suggesting that there is little to no enhancement in NO_x due to smoke.

269

270

271

272

273

274

To ensure that the observed enhancements in O₃, PM_{2.5}, CO, and ΣVOCs are consistent with known enhancements due to smoke, we calculated the observed normalized enhancement ratio (NER) of PM_{2.5} relative to CO using Eq. (2):

$$\Delta PM_{2.5} / \Delta CO = (PM_{2.5,S} - PM_{2.5,NS}) / (CO_S - CO_{NS}), \quad (2)$$

275

276

277

278

279

280

281

where $PM_{2.5,S}$ and CO_S are the daytime median PM_{2.5} and CO concentrations on the smoky weekdays, and $PM_{2.5,NS}$ and CO_{NS} are the daytime median PM_{2.5} and CO concentrations on the non-smoky weekdays (Table 1). Eq. (2) yielded a $\Delta PM_{2.5} / \Delta CO$ NER of 0.188 μg m⁻³ ppb⁻¹, which is within the range of the $\Delta PM_{2.5} / \Delta CO$ NERs of 0.057-0.228 μg m⁻³ ppb⁻¹ reported by Laing et al. (2017) for 25 smoke events in eight western U.S. cities. Therefore, the $\Delta PM_{2.5} / \Delta CO$ NER is consistent with other observations of smoke in urban areas.

Type of day or variable	N _{days}	Median O ₃ (ppb)	Median PM _{2.5} (μg m ⁻³) ^a	Median NO _x (ppb)	Median CO (ppb)	Median ΣVOCs (ppb)
Smoke	13	69.0	17.5	6.7	280.0	29.4
Non-smoke	20	61.0	10.0	6.3	240.0	19.2
p-value	N/A	< 0.05	< 0.05	0.95	< 0.05	< 0.05

282

283

284

285

286

287

288

289

290

291

292

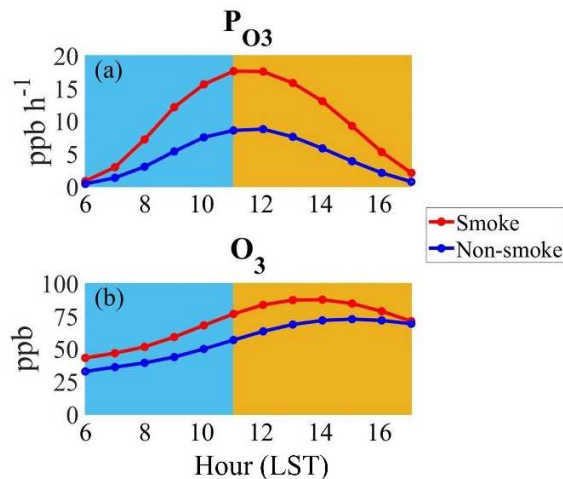
293

^aData taken from California Avenue site, which is approximately 6 km northwest of BMA.

Table 1. Statistics of observations on smoky and non-smoky weekdays Statistical summary of (1) the daytime (6:00-17:00 LST) median hourly observations of O₃, PM_{2.5}, NO_x, and CO and (2) the observed median sum of the daily-average concentrations of VOCs (ΣVOCs) at BMA on the smoky and non-smoky weekdays. The ΣVOCs values for the smoky and non-smoky weekdays were calculated by adding the concentrations shown in Table S1. P-values were determined using a 2-tailed t-test. The number of smoky and non-smoky weekdays (N_{days}) are also shown.

Model-predicted morning and afternoon P_{O3} and O₃ at BMA for the smoky and non-smoky weekdays are compared in Fig. 3. Modeled P_{O3} and O₃ were elevated on the smoky

294 weekdays, the latter being consistent with observations (Fig. 2a). Specifically, maximum P_{O_3} on
 295 the smoky and non-smoky weekdays were approximately 18 and 9 ppb h^{-1} , respectively, and
 296 maximum modeled O_3 levels on the smoky and non-smoky weekdays were about 88 and 73 ppb,
 297 respectively.
 298

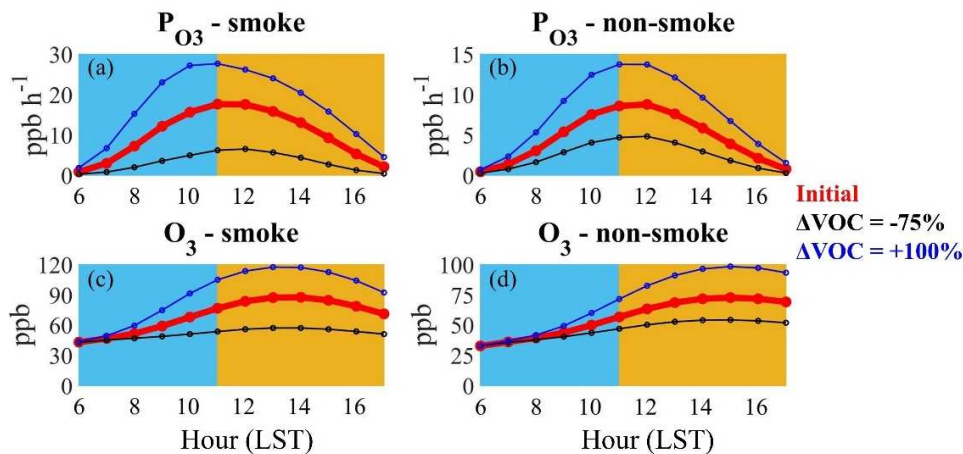


299
 300 **Fig. 3. Modeled O_3 Formation** Model-predicted (a) O_3 production rate (P_{O_3} ; ppb h^{-1}) and (b) O_3
 301 (ppb) at BMA during daytime hours (6:00-17:00 LST) on smoky and non-smoky weekdays. For
 302 ease of comparison, the daytime modeled O_3 concentrations shown in Fig. 2a are reshown in (b).
 303 The light blue and gold shading have the same meanings as in Fig. 2.
 304

305 A series of model sensitivity tests were conducted to study the impact of VOCs and NO_x
 306 on P_{O_3} and O_3 for the smoky and non-smoky weekdays. Initial and background VOC
 307 concentrations were reduced by 75% and increased by 100%, and the results of these sensitivity
 308 tests are shown in Fig. 4. On smoky weekdays, VOCs significantly impacted P_{O_3} and O_3 during
 309 morning and afternoon hours. This is because model-predicted P_{O_3} increased by up to 12 ppb h^{-1}
 310 when VOC concentrations were doubled and decreased by up to 11 ppb h^{-1} when VOC
 311 concentrations were reduced by 75%. Meanwhile, modeled hourly O_3 increased by up to 30 ppb
 312 when VOC concentrations were doubled and decreased by up to 30 ppb when VOC
 313 concentrations were reduced by 75%. Similarly, P_{O_3} and O_3 were sensitive to changes in VOC
 314 concentrations on the non-smoky weekdays, especially during the afternoon. From 11:00-17:00
 315 LST, increasing VOC values by 100% increased P_{O_3} and O_3 by up to 5 ppb h^{-1} and 26 ppb,
 316 respectively, and reducing VOC values by 75% decreased P_{O_3} and O_3 by up to 4 ppb h^{-1} and 18
 317 ppb, respectively.

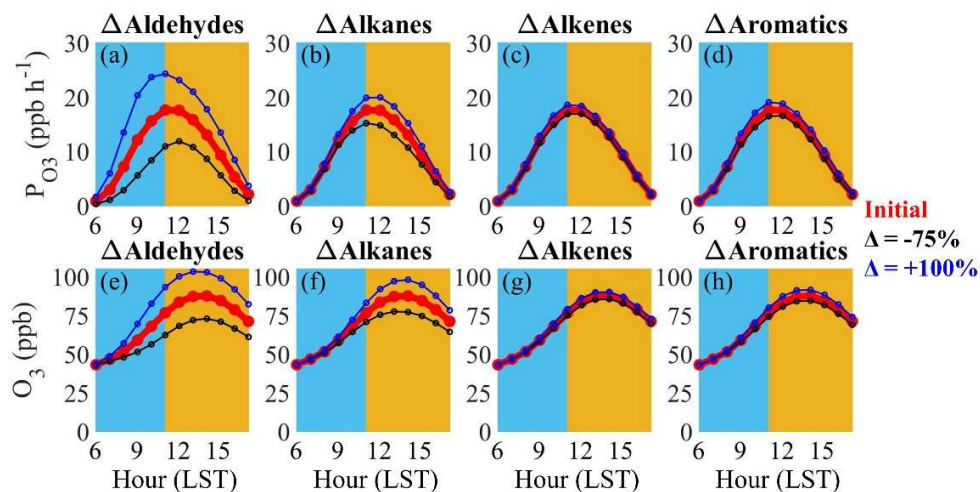
318 Additional model sensitivity tests were performed to determine which VOC class –
 319 aldehydes, alkanes, alkenes, and/or aromatics – had the greatest effect on P_{O_3} and O_3 on the
 320 smoky and non-smoky weekdays (Figs. 5 and 6). We reduced by 75% or increased by 100% the
 321 initial and background concentrations of the above VOC classes, while not changing the other
 322 model parameters. Figs. 5 and 6 indicate that aldehydes had the greatest influence on P_{O_3} and O_3
 323 on the smoky and non-smoky weekdays. The two aldehydes that had the strongest influence on
 324 O_3 were acetaldehyde (CH_3CHO) and formaldehyde ($HCHO$; Table S1). Increasing CH_3CHO
 325 and $HCHO$ concentrations by 100% led to P_{O_3} and O_3 increasing by up to 8 ppb h^{-1} and 17 ppb,
 326 respectively, on the smoky weekdays and 3 ppb h^{-1} and 10 ppb, respectively, on the non-smoky
 327 weekdays. In addition, decreasing CH_3CHO and $HCHO$ concentrations by 75% led to reductions

328 in P_{O_3} and O_3 of up to 7 ppb h^{-1} and 15 ppb , respectively, on the smoky weekdays and 2 ppb h^{-1}
 329 and 8 ppb , respectively, on the non-smoky weekdays. It is also noteworthy that CH_3CHO and
 330 HCHO had a similar impact on P_{O_3} and O_3 on the smoky weekdays (Fig. S1), and the same was
 331 true for the non-smoky weekdays (Fig. S2). The influence of CH_3CHO and HCHO on P_{O_3} and
 332 O_3 on the smoky and non-smoky weekdays is consistent with CH_3CHO and HCHO having a
 333 high OH reactivity and HCHO providing additional OH and HO_2 upon photolysis (e.g., Luecken
 334 et al., 2012, 2018).
 335

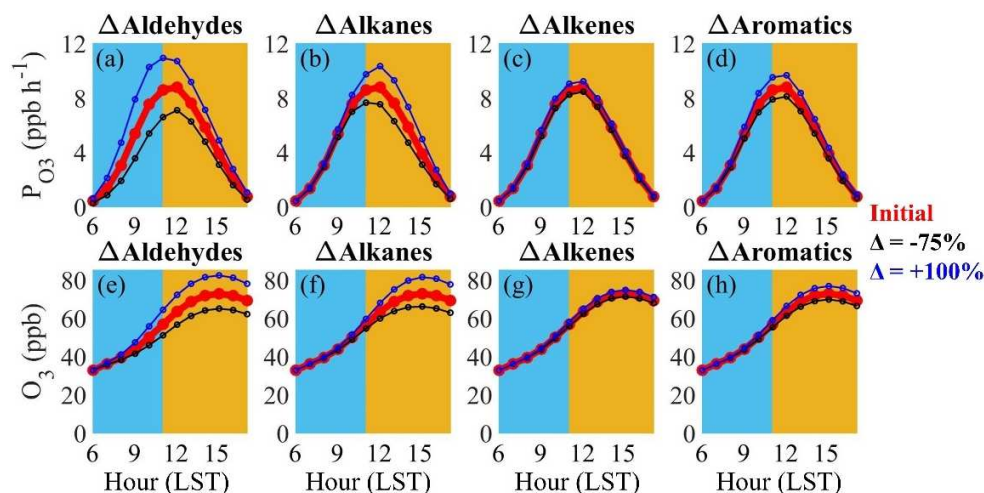


336
 337 **Fig. 4. VOC Sensitivity Tests** Model-predicted sensitivity of (a) P_{O_3} on smoky weekdays, (b)
 338 P_{O_3} on non-smoky weekdays, (c) O_3 on smoky weekdays, and (d) O_3 on non-smoky weekdays to
 339 changes in VOC concentrations. The results presented by the red and blue lines in Fig. 3 for the
 340 smoky and non-smoky weekdays, respectively, are shown in red. For the model sensitivity tests,
 341 the initial and background VOC concentrations were the only model inputs that were changed.
 342 The light blue and gold shading have the same meanings as in Fig. 2.
 343

344 Moreover, the lesser effect of alkanes, alkenes, and aromatics on O_3 production (Figs. 5-
 345 6) suggests that CH_3CHO and HCHO directly emitted from wildfires and/or anthropogenic
 346 activity had the greatest influence on P_{O_3} and O_3 , rather than the CH_3CHO and HCHO formed
 347 via oxidation from other VOC precursors (e.g., ethane, isoprene, benzene, etc.). Still, it must be
 348 noted that CH_3CHO and HCHO are short-lived, with lifetimes on the order of a few hours to one
 349 day (Jones et al., 2009; Millet et al., 2010). In addition, the large fires burning in California in
 350 July-August 2018 were located hundreds of kilometers north of BMA (Fig. 1), implying that
 351 much of the smoke affecting the site was well-aged. Therefore, some of the CH_3CHO and
 352 HCHO emitted by the fires may have undergone chemical or physical removal prior to the
 353 smoke plumes reaching BMA. This suggests that the transport of unmeasured CH_3CHO and
 354 HCHO precursors – such as methanol, ethanol, and others – may be influencing the CH_3CHO
 355 and HCHO concentrations and impacting O_3 formation on the smoky weekdays. Measurements
 356 of these species are needed at urban sites when smoke is present to either support or refute this
 357 hypothesis.
 358

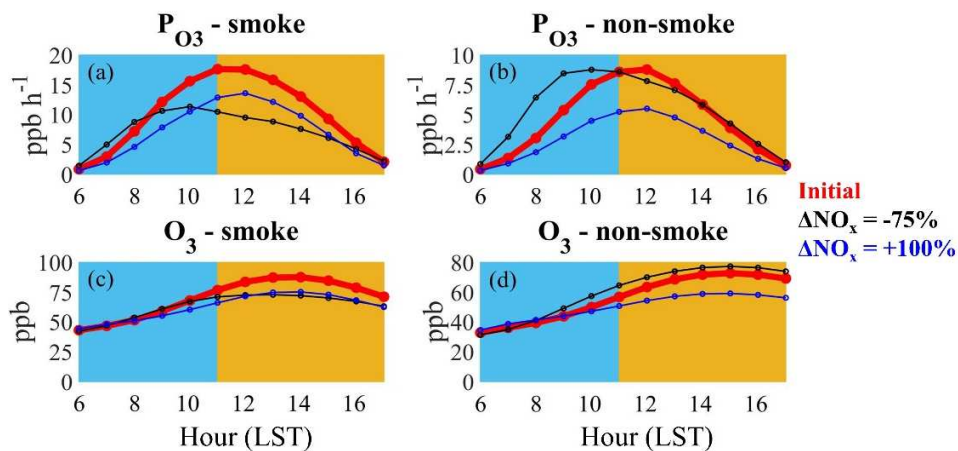


359
 360 **Fig. 5. Sensitivity Tests by VOC Class for Smoky Weekdays** Model-predicted sensitivity of
 361 P_{O_3} (top row; panels (a)-(d)) and O_3 (bottom row; panels (e)-(h)) on smoky weekdays to changes
 362 in aldehydes (leftmost column; panels (a) and (e)), alkanes (second column; panels (b) and (f)),
 363 alkenes (third column; panels (c) and (g)), and aromatics (rightmost column; panels (d) and (h)).
 364 The results presented by the red lines in Fig. 3 for smoky weekdays are shown in red. For the
 365 model sensitivity tests, the initial and background concentrations of aldehydes, alkanes, alkenes,
 366 or aromatics were the only model inputs that were changed. See Table S1 in the Supporting
 367 Information for the VOCs comprising each class. The light blue and gold shading have the same
 368 meanings as in Fig. 2.
 369



370
 371 **Fig. 6. Sensitivity Tests by VOC Class for Non-smoky Weekdays** Model-predicted sensitivity
 372 of P_{O_3} (top row; panels (a)-(d)) and O_3 (bottom row; panels (e)-(h)) on non-smoky weekdays to
 373 changes in aldehydes (leftmost column; panels (a) and (e)), alkanes (second column; panels (b)
 374 and (f)), alkenes (third column; panels (c) and (g)), and aromatics (rightmost column; panels (d)
 375 and (h)). The results presented by the blue lines in Fig. 3 for non-smoky weekdays are shown in
 376 red. For the model sensitivity tests, the initial and background concentrations of aldehydes,
 377 alkanes, alkenes, or aromatics were the only model inputs that were changed. See Table S1 in the
 378 Supporting Information for the VOCs comprising each class. The light blue and gold shading
 379 have the same meanings as in Fig. 2.

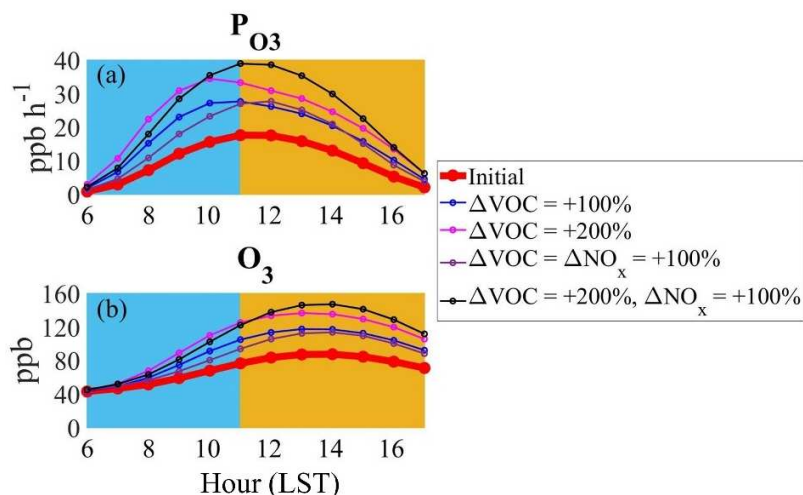
380 The sensitivity of P_{O_3} and O_3 to changes in NO_x on the smoky and non-smoky weekdays
 381 was examined by reducing and increasing initialized NO_x concentrations by 75% and 100%,
 382 respectively, without changing other model inputs (Fig. 7). On the non-smoky weekdays, P_{O_3} and
 383 O_3 were (1) relatively insensitive to NO_x when NO_x concentrations were reduced by 75% and (2)
 384 generally lower when NO_x concentrations were doubled, suggesting that the O_3 production
 385 regime at BMA on the non-smoky weekdays was likely NO_x -saturated. In contrast, afternoon P_{O_3}
 386 and O_3 decreased by up to 8 $ppb\ h^{-1}$ and 16 ppb, respectively, on the smoky weekdays after NO_x
 387 values were lowered by 75%. This result was expected given the higher VOC concentrations on
 388 smoky weekdays (Table S1). However, the lower P_{O_3} and O_3 on smoky weekdays – particularly
 389 during the afternoon hours – after increasing NO_x concentrations by 100% was unexpected. This
 390 was because we hypothesized that the O_3 production regime during wildfire smoke events would
 391 be NO_x -sensitive due to (1) the abundance of VOCs emitted by wildfires and (2) the lack of an
 392 observed enhancement in NO_x concentrations across the smoky weekdays (Fig. 2d). To further
 393 investigate this finding, Fig. 8 compares the P_{O_3} and O_3 resulting from (1) the initial simulations,
 394 (2) doubling VOCs, (3) tripling VOCs, (4) doubling VOCs and NO_x , and (5) tripling VOCs and
 395 doubling NO_x . The nearly identical P_{O_3} and O_3 after doubling VOCs versus doubling VOCs and
 396 NO_x shows that the O_3 production regime during the afternoon remained NO_x -saturated. It was
 397 not until VOC concentrations were tripled and NO_x concentrations were doubled that the
 398 afternoon P_{O_3} and O_3 exhibited behavior characteristic of a NO_x -sensitive O_3 production regime,
 399 as indicated by higher P_{O_3} and O_3 values. Figs. 7 and 8 suggest that uncertainty in the full range
 400 of VOC species is one of the largest uncertainties in our calculations of O_3 production.
 401



402
 403 **Fig. 7. NO_x Sensitivity Tests** Model-predicted sensitivity of (a) P_{O_3} on smoky weekdays, (b) P_{O_3}
 404 on non-smoky weekdays, (c) O_3 on smoky weekdays, and (d) O_3 on non-smoky weekdays to
 405 changes in NO_x . The results presented by the red and blue lines in Fig. 3 for the smoky and non-
 406 smoky weekdays, respectively, are shown in red. For the model sensitivity tests, the initialized
 407 NO_x concentrations were the only model inputs that were changed. The light blue and gold
 408 shading have the same meanings as in Fig. 2.
 409

410 The sensitivity tests described above show that P_{O_3} and O_3 are sensitive to the VOC
 411 loadings for the higher and lower concentration scenarios. Meanwhile, the response of P_{O_3} and
 412 O_3 to changes in NO_x varies (Fig. 7). On the non-smoky weekdays, P_{O_3} and O_3 are responsive to
 413 increasing NO_x concentrations and largely insensitive to decreasing NO_x concentrations. For
 414 smoky weekdays, P_{O_3} and O_3 are sensitive to lower NO_x concentrations (Fig. 7). In addition, the

415 black and magenta lines in Fig. 8 demonstrate that afternoon P_{O_3} and O_3 are responsive to higher
 416 NO_x concentrations in a manner consistent with a NO_x -sensitive O_3 production regime after VOC
 417 concentrations were tripled. Thus, we conclude that reductions in both anthropogenic NO_x and
 418 VOC concentrations are needed to lower O_3 production at BMA on typical non-smoky days.
 419 This conclusion is in line with those made by recent studies conducted in central and southern
 420 California (e.g., Nussbaumer and Cohen, 2020). However, due to the high VOC concentrations
 421 in smoke plumes, only reductions in NO_x are expected to have a significant impact on lowering
 422 O_3 concentrations on typical smoky days.
 423



424
 425 **Fig. 8. Additional Sensitivity Tests for Smoky Weekdays** Model-predicted sensitivity of (a)
 426 P_{O_3} and (b) O_3 on smoky weekdays to changes in VOCs or changes in VOCs and NO_x . The
 427 results presented by the red and blue lines in Fig. 4 for the smoky weekdays are shown in the
 428 same colors. For all model sensitivity tests, the initial and background VOC values or the initial
 429 and background VOC and the initialized NO_x values were the only model inputs that were
 430 changed. The light blue and gold shading have the same meanings as in Fig. 2.
 431

432 Two limitations regarding this study need to be discussed. First, the 24-hour time
 433 resolution and the comprehensiveness of the VOC data collected at BMA were relatively low
 434 (Table S1). Since wildfires emit hundreds of different VOCs of varying OH reactivities (e.g.,
 435 Hatch et al., 2017; Sekimoto et al., 2018), it is likely that our analysis did not fully account for
 436 the temporal variability and number of ambient VOCs at BMA. Therefore, as stated previously,
 437 the total VOC concentrations on the smoky weekdays were likely higher than the measurements
 438 presented in Table S1 indicate. The lack of a comprehensive suite of hourly measurements of
 439 VOCs known to be emitted by fires – such as furfural, methyl furfural, and dimethylfuran
 440 (Coggon et al., 2019) – likely led to an underestimate in the total VOCs present. Measurements
 441 of more fire-emitted VOCs at a higher time resolution of 1 hour would improve our ability to
 442 quantify the impact of wildfire smoke on O_3 chemistry.

443 Second, there are no formal aerosol parameterizations in F0AM, so the effect of $PM_{2.5}$ on
 444 P_{O_3} and O_3 could not be investigated. Although previous studies have explored the relationship
 445 between $PM_{2.5}$ and O_3 during smoke events (e.g., Baker et al., 2016; Buysse et al.,
 446 2019), the influence of interactive aerosol chemistry (i.e., gas-particle reactions, phase
 447 partitioning, thermodynamic equilibrium, etc.) on O_3 during urban smoke events has yet to be
 448 elucidated. Since aerosols can act as a radical sink (e.g., Emmerson et al., 2007; Stone et al.,

449 2012) and thus inhibit O₃ formation, investigating the impact of interactive aerosol chemistry on
450 O₃ production during smoke events in urban areas should be a focus of future studies.

451

452 **4. Conclusions**

453

454 This study assessed the effect of wildfire smoke on O₃ production at the urban
455 Bakersfield Municipal Airport (BMA) site in California across 13 smoky weekdays and 20 non-
456 smoky weekdays in summer 2018. Median surface observations for the smoky and non-smoky
457 weekdays revealed that afternoon O₃ typically reached values up to 79 and 73 ppb, respectively,
458 and morning and afternoon O₃ were largely influenced by local photochemistry. The observed
459 median concentrations of PM_{2.5}, CO, and ΣVOCs were lower on non-smoky weekdays compared
460 to smoky weekdays. Meanwhile, observed daytime median NO_x concentrations were almost
461 identical for the smoky and non-smoky weekdays, indicating that the smoke plumes contained a
462 negligible amount of NO_x. Box model simulations showed that simultaneous reductions in
463 anthropogenic VOCs and NO_x will likely be the best approach for decreasing P_{O₃} and O₃ on
464 typical non-smoky days at BMA. For typical smoky days, only anthropogenic NO_x controls are
465 expected to significantly reduce O₃ levels due to the high concentrations of VOCs in smoke
466 plumes.

467 To further investigate the influence of wildfire smoke on O₃ production at BMA and
468 other urban sites, future work needs to be conducted in the following areas:

469

- 470 1. Make hourly measurements of more fire-emitted VOCs.
- 471 2. Assess the impact of interactive aerosol chemistry on O₃ production.
- 472 3. Examine individual smoke cases at BMA that are characterized by variable plume age,
473 plume composition, and meteorology (i.e., air mass origin, temperature, etc.).

474

475 Addressing the above areas of future research may improve the understanding of urban O₃
476 production during smoke-influenced periods.

477

478 **Declaration of interests**

479

480 The authors declare that they have no known competing financial interests or personal
481 relationships that could have appeared to influence the work reported in this paper.

482

483 **Acknowledgements**

484

485 This work was supported by the National Oceanic and Atmospheric Administration (NOAA;
486 grant number NA17OAR431001).

487

488 **References**

489

490 Akagi, S.K., Yokelson, R.J., Wiedinmyer, C., Alvarado, M.J., Reid, J.S., Karl, T., Crouse, J.D.,
491 Wennberg, P.O., 2011. Emission factors for open and domestic biomass burning for use
492 in atmospheric models. *Atmos. Chem. Phys.*, 11, 4039-4072. [https://doi.org/10.5194/acp-](https://doi.org/10.5194/acp-11-4039-2011)
493 11-4039-2011

494 Aldersley, A., Murray, S.J., Cornell, S.E., 2011. Global and regional analysis of climate and
495 human drivers of wildfire. *Sci. Total Environ.*, 409, 3472-3481.
496 <https://doi.org/10.1016/j.scitotenv.2011.05.032>

497 Alvarado, M.J., Lonsdale, C.R., Yokelson, R.J., Akagi, S.K., Coe, H., Craven, J.S., Fischer,
498 E.V., McMeeking, G.R., Seinfeld, J.H., Soni, T., Taylor, J.W., Weise, D.R., Wold, C.E.,
499 2015. Investigating the links between ozone and organic aerosol chemistry in a biomass
500 burning plume from a prescribed fire in California chaparral. *Atmos. Chem. Phys.*, 15,
501 6667-6688. <https://doi.org/10.5194/acp-15-6667-2015>

502 Andreae, M.O., 2019. Emission of trace gases and aerosols from biomass burning – an updated
503 assessment. *Atmos. Chem. Phys.*, 19, 8523-8546. [https://doi.org/10.5194/acp-19-8523-](https://doi.org/10.5194/acp-19-8523-2019)
504 2019

505 Baidar, S., Hardesty, R.M., Kim, S.-W., Langford, A.O., Oetjen, H., Senff, C.J., Trainer, M.,
506 Volkamer, R., 2015. Weakening of the weekend ozone effect over California's South
507 Coast Air Basin. *Geophys. Res. Lett.*, 42, 9457-9464.
508 <https://doi.org/10.1002/2015GL066419>

509 Baker, K.R., Woody, M.C., Tonnesen, G.S., Hutzell, W., Pye, H.O.T., Beaver, M.R., Pouliot, G.,
510 Pierce, T., 2016. Contribution of regional-scale fire events to ozone and PM_{2.5} air quality
511 estimated by photochemical modeling approaches. *Atmos. Environ.*, 140, 539-554.
512 <https://doi.org/10.1016/j.atmosenv.2016.06.032>

513 Balch, J.K., Bradley, B.A., Abatzoglou, J.T., Nagy, R.C., Fusco, E.J., Mahood, A.L., 2017.
514 Human-started wildfires expand the fire niche across the United States. *Proc. Natl. Acad.*
515 *Sci. U.S.A.*, 114, 2946-2951. <https://doi.org/10.1073/pnas.1617394114>

516 Baylon, P., Jaffe, D.A., Hall, S.R., Ullmann, K., Alvarado, M.J., Lefer, B.L., 2018. Impact of
517 Biomass Burning Plumes on Photolysis Rates and Ozone Formation at the Mount
518 Bachelor Observatory. *J. Geophys. Res.: Atmos.*, 123, 2272-2284.
519 <https://doi.org/10.1002/2017JD027341>

520 Blanchard, C.L., Tanenbaum, S.J., 2003. Differences between Weekday and Weekend Air
521 Pollutant Levels in Southern California. *J. Air Waste Manage. Assoc.*, 53, 816-828.
522 <https://doi.org/10.1080/10473289.2003.10466222>

523 Bloss, C., Wagner, V., Jenkin, M.E., Volkamer, R., Bloss, W.J., Lee, J.D., Heard, D.E., Wirtz,
524 K., Martin-Reviejo, M., Rea, G., Wenger, J.C., Pilling, M.J., 2005. Development of a
525 detailed chemical mechanism (MCMv3.1) for the atmospheric oxidation of aromatic
526 hydrocarbons. *Atmos. Chem. Phys.*, 5, 641-664. <https://doi.org/10.5194/acp-5-641-2005>

527 Buysse, C.E., Kaulfus, A., Nair, U., Jaffe, D.A., 2019. Relationships between Particulate Matter,
528 Ozone, and Nitrogen Oxides during Urban Smoke Events in the Western US. *Environ.*
529 *Sci. Technol.*, 53, 12519-12528. <https://doi.org/10.1021/acs.est.9b05241>

530 Cai, C., Kulkarni, S., Zhao, Z., Kaduwela, A.P., Avise, J.C., DaMassa, J.A., Singh, H.B.,
531 Weinheimer, A.J., Cohen, R.C., Diskin, G.S., Wennberg, P., Dibb, J.E., Huey, G.,
532 Wisthaler, A., Jimenez, J.L., Cubison, M.J., 2016. Simulating reactive nitrogen, carbon
533 monoxide, and ozone in California during ARCTAS-CARB 2008 with high wildfire
534 activity. *Atmos. Environ.*, 128, 28-44. <https://doi.org/10.1016/j.atmosenv.2015.12.031>

535 Camalier, L., Cox, W., Dolwick, P., 2007. The effects of meteorology on ozone in urban areas
536 and their use in assessing ozone trends. *Atmos. Environ.*, 41, 7127-7137.
537 <https://doi.org/10.1016/j.atmosenv.2007.04.061>

538 Coggon, M.M., Lim, C.Y., Koss, A.R., Sekimoto, K., Yuan, B., Gilman, J.B., Hagan, D.H.,
539 Selimovic, V., Zarzana, K.J., Brown, S.S., Roberts, J.M., Müller, M., Yokelson, R.,

540 Wisthaler, A., Krechmer, J.E., Jimenez, J.L., Cappa, C., Kroll, J.H., de Gouw, J.,
541 Warneke, C., 2019. OH chemistry of non-methane organic gases (NMOGs) emitted from
542 laboratory and ambient biomass burning smoke: evaluating the influence of furans and
543 oxygenated aromatics on ozone and secondary NMOG formation. *Atmos. Chem. Phys.*,
544 19, 14875-14899. <https://doi.org/10.5194/acp-19-14875-2019>

545 de Foy, B., Brune, W.H., Schauer, J.J., 2020. Changes in ozone photochemical regime in Fresno,
546 California from 1994 to 2018 deduced from changes in the weekend effect. *Environ.*
547 *Pollut.*, 263, 114380. <https://doi.org/10.1016/j.envpol.2020.114380>

548 Decker, Z.C.J., Zarzana, K.J., Coggon, M., Min, K.-E., Pollack, I., Ryerson, T.B., Peischl, J.,
549 Edwards, P., Dubé, W.P., Markovic, M.Z., Roberts, J.M., Veres, P.R., Graus, M.,
550 Warneke, C., de Gouw, J., Hatch, L.E., Barsanti, K.C., Brown, S.S., 2019. Nighttime
551 Chemical Transformation in Biomass Burning Plumes: A Box Model Analysis Initialized
552 with Aircraft Observations. *Environ. Sci. Technol.*, 53, 2529-2538.
553 <https://doi.org/10.1021/acs.est.8b05359>

554 Dennison, P.E., Brewer, S.C., Arnold, J.D., Moritz, M.A., 2014. Large wildfire trends in the
555 western United States, 1984-2011. *Geophys. Res. Lett.*, 41, 2928-2933.
556 <https://doi.org/10.1002/2014GL059576>

557 Dreessen, J., Sullivan, J., Delgado, R., 2016. Observations and impacts of transported Canadian
558 wildfire smoke on ozone and aerosol air quality in the Maryland region on June 9-12,
559 2015. *J. Air Waste Manage. Assoc.*, 66, 842-862.
560 <https://doi.org/10.1080/10962247.2016.1161674>

561 Emmerson, K.M., Carslaw, N., Carslaw, D.C., Lee, J.D., McFiggans, G., Bloss, W.J.,
562 Gravestock, T., Heard, D.E., Hopkins, J., Ingham, T., Pilling, M.J., Smith, S.C., Jacob,
563 M., Monks, P.S., 2007. Free radical modelling studies during the UK TORCH Campaign
564 in Summer 2003. *Atmos. Chem. Phys.*, 7, 167-181. [https://doi.org/10.5194/acp-7-167-](https://doi.org/10.5194/acp-7-167-2007)
565 [2007](https://doi.org/10.5194/acp-7-167-2007)

566 Farmer, D.K., Perring, A.E., Wooldridge, P.J., Blake, D.R., Baker, A., Meinardi, S., Huey, L.G.,
567 Tanner, D., Vargas, O., Cohen, R.C., 2011. Impact of organic nitrates on urban ozone
568 production. *Atmos. Chem. Phys.*, 11, 4085-4094. [https://doi.org/10.5194/acp-11-4085-](https://doi.org/10.5194/acp-11-4085-2011)
569 [2011](https://doi.org/10.5194/acp-11-4085-2011)

570 Fujita, E.M., Stockwell, W.R., Campbell, D.E., Keislar, R.E., Lawson, D.R., 2003. Evolution of
571 the Magnitude and Spatial Extent of the Weekend Ozone Effect in California's South
572 Coast Air Basin, 1981-2000. *J. Air Waste Manage. Assoc.*, 53, 802-815.
573 <https://doi.org/10.1080/10473289.2003.10466225>

574 Gong, X., Kaulfus, A., Nair, U., Jaffe, D.A., 2017. Quantifying O₃ Impacts in Urban Areas Due
575 to Wildfires Using a Generalized Additive Model. *Environ. Sci. Technol.*, 51, 13216-
576 13223. <https://doi.org/10.1021/acs.est.7b03130>

577 Hatch, L.E., Yokelson, R.J., Stockwell, C.E., Veres, P.R., Simpson, I.J., Blake, D.R., Orlando,
578 J.J., Barsanti, K.C., 2017. Multi-instrument comparison and compilation of non-methane
579 organic gas emissions from biomass burning and implications for smoke-derived
580 secondary organic aerosol precursors. *Atmos. Chem. Phys.*, 17, 1471-1489.
581 <https://doi.org/10.5194/acp-17-1471-2017>

582 IEM, 2021. Iowa Environmental Mesonet: ASOS-AWOS-METAR Data Download. URL:
583 <https://mesonet.agron.iastate.edu/request/download.phtml>, Accessed Date: 20 January
584 2021.

585 Jaffe, D., Bertschi, I., Jaeglé, L., Novelli, P., Reid, J.S., Tanimoto, H., Vingarzan, R., Westphal,
586 D.L., 2004. Long-range transport of Siberian biomass burning emissions and impact on
587 surface ozone in western North America. *Geophys. Res. Lett.*, 31, L16106.
588 <https://doi.org/10.1029/2004GL020093>

589 Jaffe, D.A., Wigder, N., Downey, N., Pfister, G., Boynard, A., Reid, S.B., 2013. Impact of
590 Wildfires on Ozone Exceptional Events in the Western U.S. *Environ. Sci. Technol.*, 47,
591 11065-11072. <https://doi.org/10.1021/es402164f>

592 Jenkin, M.E., Saunders, S.M., Pilling, M.J., 1997. The tropospheric degradation of volatile
593 organic compounds: a protocol for mechanism development. *Atmos. Environ.*, 31, 81-
594 104. [https://doi.org/10.1016/S1352-2310\(96\)00105-7](https://doi.org/10.1016/S1352-2310(96)00105-7)

595 Jenkin, M.E., Saunders, S.M., Wagner, V., Pilling, M.J., 2003. Protocol for the development of
596 the Master Chemical Mechanism, MCM v3 (Part B): tropospheric degradation of
597 aromatic volatile organic compounds. *Atmos. Chem. Phys.*, 3, 181-193.
598 <https://doi.org/10.5194/acp-3-181-2003>

599 Jenkin, M.E., Young, J.C., Rickard, A.R., 2015. The MCM v3.3.1 degradation scheme for
600 isoprene. *Atmos. Chem. Phys.*, 15, 11433-11459. [https://doi.org/10.5194/acp-15-11433-](https://doi.org/10.5194/acp-15-11433-2015)
601 [2015](https://doi.org/10.5194/acp-15-11433-2015)

602 Jones, N.B., Riedel, K., Allan, W., Wood, S., Palmer, P.I., Chance, K., Notholt, J., 2009. Long-
603 term tropospheric formaldehyde concentrations deduced from ground-based fourier
604 transform solar infrared measurements. *Atmos. Chem. Phys.*, 9, 7131-7142. [www.atmos-](http://www.atmos-chem-phys.net/9/7131/2009)
605 [chem-phys.net/9/7131/2009](http://www.atmos-chem-phys.net/9/7131/2009)

606 Kitzberger, T., Brown, P.M., Heyerdahl, E.K., Swetnam, T.W., Veblen, T.T., 2007. Contingent
607 Pacific-Atlantic Ocean influence on multicentury wildfire synchrony over western North
608 America. *Proc. Natl. Acad. Sci. U.S.A.*, 104, 543-548.
609 <https://doi.org/10.1073/pnas.0606078104>

610 Laing, J.R., Jaffe, D.A., 2019. Wildfires Are Causing Extreme PM Concentrations in the
611 Western United States. *EM*, June 2019, 18-23.

612 Laing, J.R., Jaffe, D.A., Slavens, A.P., Li, W., Wang, W., 2017. Can $\Delta\text{PM}_{2.5}/\Delta\text{CO}$ and
613 $\Delta\text{NO}_y/\Delta\text{CO}$ Enhancement Ratios Be Used to Characterize the Influence of Wildfire
614 Smoke in Urban Areas? *Aerosol Air Qual. Res.*, 17, 2413-2423.
615 <https://doi.org/10.4209/aaqr.2017.02.0069>

616 Lindaas, J., Farmer, D.K., Pollack, I.B., Abeleira, A., Flocke, F., Roscioli, R., Herndon, S.,
617 Fischer, E.V., 2017. Changes in ozone and precursors during two aged wildfire smoke
618 events in the Colorado Front Range in summer 2015. *Atmos. Chem. Phys.*, 17, 10691-
619 10707. <https://doi.org/10.5194/acp-17-10691-2017>

620 Lindaas, J., Pollack, I.B., Garofalo, L.A., Pothier, M.A., Farmer, D.K., Kreidenweis, S.M.,
621 Campos, T.L., Flocke, F., Weinheimer, A.J., Montzka, D.D., Tyndall, G.S., Palm, B.B.,
622 Peng, Q., Thornton, J.A., Permar, W., Wielgasz, C., Hu, L., Ottmar, R.D., Restaino, J.C.,
623 Hudak, A.T., Ku, I.-T., Zhou, Y., Sive, B.C., Sullivan, A., Collett Jr., J.L., Fischer, E.V.,
624 2020. Emissions of Reactive Nitrogen From Western U.S. Wildfires During Summer
625 2018. *J. Geophys. Res.: Atmos.*, 125, e2020JD032657.
626 <https://doi.org/10.1029/2020JD032657>

627 Littell, J.S., McKenzie, D., Peterson, D.L., Westerling, A.L., 2009. Climate and wildfire area
628 burned in western U.S. ecoprovinces, 1916-2003. *Ecol. Appl.*, 19, 1003-1021.
629 <https://doi.org/10.1890/07-1183.1>

630 Lu, X., Zhang, L., Yue, X., Zhang, J., Jaffe, D.A., Stohl, A., Zhao, Y., Shao, J., 2016. Wildfire
631 influences on the variability and trend of summer surface ozone in the mountainous
632 western United States. *Atmos. Chem. Phys.*, 16, 14687-14702.
633 <https://doi.org/10.5194/acp-16-14687-2016>

634 Luecken, D.J., Hutzell, W.T., Strum, M.L., Pouliot, G.A., 2012. Regional sources of atmospheric
635 formaldehyde and acetaldehyde, and implications for atmospheric modeling. *Atmos.*
636 *Environ.*, 47, 477-490. <https://doi.org/10.1016/j.atmosenv.2011.10.005>

637 Luecken, D.J., Napelenok, S.L., Strum, M., Scheffe, R., Phillips, S., 2018. Sensitivity of
638 Ambient Atmospheric Formaldehyde and Ozone to Precursor Species and Source Types
639 Across the United States. *Environ. Sci. Technol.*, 52, 4668-4675.
640 <https://doi.org/10.1021/acs.est.7b05509>

641 Mason, S.A., Trentmann, J., Winterrath, T., Yokelson, R.J., Christian, T.J., Carlson, L.J.,
642 Warner, T.R., Wolfe, L.C., Andreae, M.O., 2006. Intercomparison of Two Box Models
643 of the Chemical Evolution in Biomass-Burning Smoke Plumes. *J. Atmos. Chem.*, 55,
644 273-297. <https://doi.org/10.1007/s10874-006-9039-5>

645 McClure, C.D., Jaffe, D.A., 2018a. US particulate matter air quality improves except in wildfire-
646 prone areas. *Proc. Natl. Acad. Sci. U.S.A.*, 115, 7901-7906.
647 <https://doi.org/10.1073/pnas.1804353115>

648 McClure, C.D., Jaffe, D.A., 2018b. Investigation of high ozone events due to wildfire smoke in
649 an urban area. *Atmos. Environ.*, 194, 146-157.
650 <https://doi.org/10.1016/j.atmosenv.2018.09.021>

651 McDuffie, E.E., Edwards, P.M., Gilman, J.B., Lerner, B.M., Dubé, W.P., Trainer, M., Wolfe,
652 D.E., Angevine, W.M., deGouw, J., Williams, E.J., Tevlin, A.G., Murphy, J.G., Fischer,
653 E.V., McKeen, S., Ryerson, T.B., Peischl, J., Holloway, J.S., Aikin, K., Langford, A.O.,
654 Senff, C.J., Alvarez II, R.J., Hall, S.R., Ullmann, K., Lantz, K.O., Brown, S.S., 2016.
655 Influence of oil and gas emissions on summertime ozone in the Colorado Northern Front
656 Range. *J. Geophys. Res.: Atmos.*, 121, 8712-8729.
657 <https://doi.org/10.1002/2016JD025265>

658 Miller, J.D., Safford, H., 2012. Trends in Wildfire Severity: 1984 to 2010 in the Sierra Nevada,
659 Modoc Plateau, and Southern Cascades, California, USA. *Fire Ecol.*, 8, 41-57.
660 <https://doi.org/10.4996/fireecology.0803041>

661 Millet, D.B., Guenther, A., Siegel, D.A., Nelson, N.B., Singh, H.B., de Gouw, J.A., Warneke, C.,
662 Williams, J., Eerdekens, G., Sinha, V., Karl, T., Flocke, F., Apel, E., Riemer, D.D.,
663 Palmer, P.I., Barkley, M., 2010. Global atmospheric budget of acetaldehyde: 3-D model
664 analysis and constraints from in-situ and satellite observations. *Atmos. Chem. Phys.*, 10,
665 3405-3425. www.atmos-chem-phys.net/10/3405/2010

666 Moritz, M.A., Parisien, M.-A., Batllori, E., Krawchuk, M.A., Van Dorn, J., Ganz, D.J., Hayhoe,
667 K., 2012. Climate change and disruptions to global fire activity. *Ecosphere*, 3, 1-22.
668 <https://doi.org/10.1890/ES11-00345.1>

669 Müller, M., Anderson, B.E., Beyersdorf, A.J., Crawford, J.H., Diskin, G.S., Eichler, P., Fried, A.,
670 Keutsch, F.N., Mikoviny, T., Thornhill, K.L., Walega, J.G., Weinheimer, A.J., Yang, M.,
671 Yokelson, R.J., Wisthaler, A., 2016. In situ measurements and modeling of reactive trace
672 gases in a small biomass burning plume. *Atmos. Chem. Phys.*, 16, 3813-3824.
673 <https://doi.org/10.5194/acp-16-3813-2016>

674 Ninneman, M., Lu, S., Zhou, X., Schwab, J., 2020. On the Importance of Surface-Enhanced
675 Renoxification as an Oxides of Nitrogen Source in Rural and Urban New York State.

676 ACS Earth Space Chem., 4, 1985-1992.
677 <https://doi.org/10.1021/acsearthspacechem.0c00185>
678 Nussbaumer, C.M., Cohen, R.C., 2020. The Role of Temperature and NO_x in Ozone Trends in
679 the Los Angeles Basin. *Environ. Sci. Technol.*, 54, 15652-15659.
680 <https://dx.doi.org/10.1021/acs.est.0c04910>
681 Pechony, O., Shindell, D.T., 2010. Driving forces of global wildfires over the past millennium
682 and the forthcoming century. *Proc. Natl. Acad. Sci. U.S.A.*, 107, 19167-19170.
683 <https://doi.org/10.1073/pnas.1003669107>
684 Pusede, S.E., Cohen, R.C., 2012. On the observed response of ozone to NO_x and VOC reactivity
685 reductions in San Joaquin Valley California 1995-present. *Atmos. Chem. Phys.*, 12,
686 8323-8339. <https://doi.org/10.5194/acp-12-8323-2012>
687 Qian, Y., Henneman, L.R.F., Mulholland, J.A., Russell, A.G., 2019. Empirical Development of
688 Ozone Isopleths: Applications to Los Angeles. *Environ. Sci. Technol. Lett.*, 6, 294-299.
689 <https://doi.org/10.1021/acs.estlett.9b00160>
690 Rubio, M.A., Lissi, E., Gramsch, E., Garreaud, R., 2015. Effect of Nearby Forest Fires on
691 Ground Level Ozone Concentrations in Santiago, Chile. *Atmosphere*, 6, 1926-1938.
692 <https://doi.org/10.3390/atmos6121838>
693 Saunders, S.M., Jenkin, M.E., Derwent, R.G., Pilling, M.J., 2003. Protocol for the development
694 of the Master Chemical Mechanism, MCM v3 (Part A): tropospheric degradation of non-
695 aromatic volatile organic compounds. *Atmos. Chem. Phys.*, 3, 161-180.
696 <https://doi.org/10.5194/acp-3-161-2003>
697 Sekimoto, K., Koss, A.R., Gilman, J.B., Selimovic, V., Coggon, M.M., Zarzana, K.J., Yuan, B.,
698 Lerner, B.M., Brown, S.S., Warneke, C., Yokelson, R.J., Roberts, J.M., de Gouw, J.,
699 2018. High- and low-temperature pyrolysis profiles describe volatile organic compound
700 emissions from western US wildfire fuels. *Atmos. Chem. Phys.*, 18, 9263-9281.
701 <https://doi.org/10.5194/acp-18-9263-2018>
702 Sillman, S., 1999. The relation between ozone, NO_x and hydrocarbons in urban and polluted
703 rural environments. *Atmos. Environ.*, 33, 1821-1845. [https://doi.org/10.1016/S1352-](https://doi.org/10.1016/S1352-2310(98)00345-8)
704 [2310\(98\)00345-8](https://doi.org/10.1016/S1352-2310(98)00345-8)
705 Singh, H.B., Cai, C., Kaduwela, A., Weinheimer, A., Wisthaler, A., 2012. Interactions of fire
706 emissions and urban pollution over California: Ozone formation and air quality
707 simulations. *Atmos. Environ.*, 56, 45-51. <https://doi.org/10.1016/j.atmosenv.2012.03.046>
708 Spracklen, D.V., Mickley, L.J., Logan, J.A., Hudman, R.C., Yevich, R., Flannigan, M.D.,
709 Westerling, A.L., 2009. Impacts of climate change from 2000 to 2050 on wildfire activity
710 and carbonaceous aerosol concentrations in the western United States. *J. Geophys. Res.:*
711 *Atmos.*, 114, D20301. <https://doi.org/10.1029/2008JD010966>
712 Stone, D., Whalley, L.K., Heard, D.E., 2012. Tropospheric OH and HO₂ radicals: field
713 measurements and model comparisons. *Chem. Soc. Rev.*, 41, 6348-6404.
714 <https://doi.org/10.1039/C2CS35140D>
715 Thornton, J.A., Wooldridge, P.J., Cohen, R.C., Martinez, M., Harder, H., Brune, W.H.,
716 Williams, E.J., Roberts, J.M., Fehsenfeld, F.C., Hall, S.R., Shetter, R.E., Wert, B.P.,
717 Fried, A., 2002. Ozone production rates as a function of NO_x abundances and HO_x
718 production rates in the Nashville urban plume. *J. Geophys. Res.: Atmos.*, 107, ACH 7-1-
719 ACH 7-17. <https://doi.org/10.1029/2001JD000932>
720 U.S. Environmental Protection Agency (U.S. EPA), 2016. Guidance on the Preparation of
721 Exceptional Events Demonstrations for Wildfire Events that May Influence Ozone

722 Concentrations. URL: [https://www.epa.gov/sites/production/files/2016-](https://www.epa.gov/sites/production/files/2016-09/documents/exceptional_events_guidance_9-16-16_final.pdf)
723 [09/documents/exceptional_events_guidance_9-16-16_final.pdf](https://www.epa.gov/sites/production/files/2016-09/documents/exceptional_events_guidance_9-16-16_final.pdf), Accessed date: 15 April
724 2021.

725 Val Martin, M., Heald, C.L., Lamarque, J.-F., Tilmes, S., Emmons, L.K., Schichtel, B.A., 2015.
726 How emissions, climate, and land use change will impact mid-century air quality over the
727 United States: a focus on effects at national parks. *Atmos. Chem. Phys.*, 15, 2805-2823.
728 <https://doi.org/10.5194/acp-15-2805-2015>

729 Westerling, A.L., Hidalgo, H.G., Cayan, D.R., Swetnam, T.W., 2006. Warming and Earlier
730 Spring Increase Western U.S. Forest Wildfire Activity. *Science*, 313, 940-943.
731 <https://doi.org/10.1126/science.1128834>

732 Wolfe, G., 2020. Overview of the Framework for 0-D Atmospheric Modeling (F0AM) Version
733 4.0. URL: https://github.com/AirChem/F0AM/blob/master/F0AM_UserManual.pdf,
734 Accessed date: 29 August 2020.

735 Wolfe, G.M., Marvin, M.R., Roberts, S.J., Travis, K.R., Liao, J., 2016. The Framework for 0-D
736 Atmospheric Modeling (F0AM) v3.1. *Geosci. Model Dev.*, 9, 3309-3319.
737 <https://doi.org/10.5194/gmd-9-3309-2016>

738 Zhang, L., Jacob, D.J., Yue, X., Downey, N.V., Wood, D.A., Blewitt, D., 2014. Sources
739 contributing to background surface ozone in the US Intermountain West. *Atmos. Chem.*
740 *Phys.*, 14, 5295-5309. <https://doi.org/10.5194/acp-14-5295-2014>